Severe Wave-Body Interactions: a Potential-Flow HPC Method and its Strong Domain-Decomposition Coupling with a Level-Set Navier-Stokes Solver

Finn-Christian W. Hanssen*[1], Giuseppina Colicchio[1,2], Marilena Greco[1,2]

[1]NTNU AMOS, Marine Technology Department, NTNU, Trondheim, Norway
[2]CNR-INM, Institute of Marine Engineering, Rome, Italy
*finnchri83@gmail.com

1 INTRODUCTION

The main objective of our ongoing research is to investigate wave loads on and motions of floating bodies in steep waves. For modelling non-linear water-wave and wave-body interaction problems, researchers can use two main classes of numerical methods, where the preferred choice depends on the features of the problem. One class consists of potential-flow solvers, which are efficient and accurate in simulating propagating waves. In this framework, we have proposed a method based on the high-order harmonic polynomial cell (HPC) method at the 32nd IWWWFB. In [1], its ability to simulate a variety of wave-propagation problems has been demonstrated in detail, even for steep waves close to breaking. The other class consists of more computationally expensive Navier-Stokes solvers, able to deal with problems involving wave breaking and fragmentation phenomena and/or important viscous effects. To benefit from the strengths of both classes of solvers, couplings between potential-flow and Navier-Stokes solvers have received increased attention in the research community during the last years. In this framework, in [2], we proposed a 2D strong Domain-Decomposition (DD) strategy between a Level-Set Navier-Stokes (LS-NS) solver and a non-linear potential-flow solver based on the boundary element method (BEM) to analyze a dam-breaking problem and subsequent wave impact on a vertical wall. Here, the HPC-based potential-flow (HPC-PF) solver's capability to handle wave-body interactions, when viscous effects are limited, is documented by comparing against the BEM and available experiments. Then, a 2D strong DD strategy between the HPC-PF solver and the LS-NS solver is proposed to handle more general scenarios and enhancing accuracy and efficiency with respect to using the BEM solver.

2 POTENTIAL-FLOW FRAMEWORK

Here, the HPC-PF solver is briefly described and compared with the mentioned BEM solver for a wave-body interaction problem with a freely floating body.

2.1 HPC Solver

The original HPC method was proposed by Shao & Faltinsen [4] as an accurate and efficient method to solve the Laplace equation for the velocity potential. The computational domain is divided into overlapping quadrilateral cells, where the velocity potential in a point with global coordinates (y_p, z_p) located within a cell is represented as a linear combination of harmonic polynomials:

$$\varphi(y_p, z_p) = \sum_{i=1}^{8} \sum_{j=1}^{8} c_{j,i} f_j(\bar{y}_p, \bar{z}_p)\, \varphi_i. \tag{1}$$

$(\bar{y}_p, \bar{z}_p)$ are here local coordinates in the cell coordinate system. Each cell consists of eight boundary nodes, so that harmonic polynomials f_j up to 4th order are included in eq. (1). This gives the method a spatial accuracy of between 3rd and 4th order. Using eq. (1), the Laplace equation is automatically satisfied and the boundary-value problem (BVP) for φ can be solved by enforcing Dirichlet and/or Neumann conditions along the boundaries of the fluid domain. Ma et al. [5] demonstrated that, in order to achieve the highest possible accuracy in the HPC method, square cells are preferred. In the present work, square cells are used throughout, and the free surface is modelled as an immersed boundary in a Cartesian grid. The time evolution of the free surface is tracked by following markers, and eq. (1) is used to impose Dirichlet conditions for the velocity potential on the free surface

with ghost nodes located outside the fluid domain. The velocity in any point inside the fluid is determined by taking the gradient of eq. (1) in a cell that contains the point. The fluid pressure is found from the Bernoulli equation,

$$p(y,z,t) = -\rho\left(\varphi_t + \frac{1}{2}|\nabla\varphi|^2 + gz\right), \tag{2}$$

where the pressure is defined as zero on the free surface. The time derivative φ_t in the fluid is determined by solving an auxiliary BVP similar to that for φ. The additional computational cost in doing so is limited, since the two problems share the same global coefficient matrix.

2.2 Wave-Floating Body Interactions: Study Case

The freely floating 2D ship section in regular deep-water waves in Fig. 1 is considered. A 4th order Runge-Kutta scheme, similar to that in [1], is used to march the solution in time. The ship section is modelled as an immersed boundary in a body-fixed, overlapping grid similar to what we proposed at the 32nd IWWWFB.

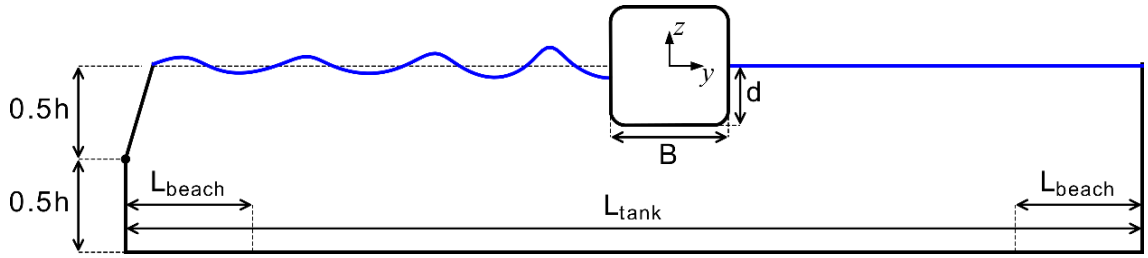

Fig. 1 Wave tank with water depth h with a freely floating ship section with breadth B and draught d. L_{tank} and L_{beach} are the lengths of tank and numerical damping zones, respectively. Details of the test case are found in e.g. [6] and [7].

Transfer functions for 1st order motions in sway, heave and roll are shown in Fig. 2 for an incident wave amplitude ζ_A = 0.035 m. The HPC results are compared to a linear solution from [6], the experimental results from [7] and the BEM. In each plot, the motion time series are compared with the BEM solution for two wave frequencies with large (1) and moderate (2) 1st order motions, respectively. For ξ_B = 1.0, where 1st order motions are moderate, the non-linear HPC and BEM results agree well with linear and experimental results. Close to heave and roll resonance at ξ_B = 0.5, their solutions deviate from linear theory and experiments. Due to the large motions, we can expect non-linear and viscous effects to be important. The HPC results compare well with the BEM throughout, even close to resonance.

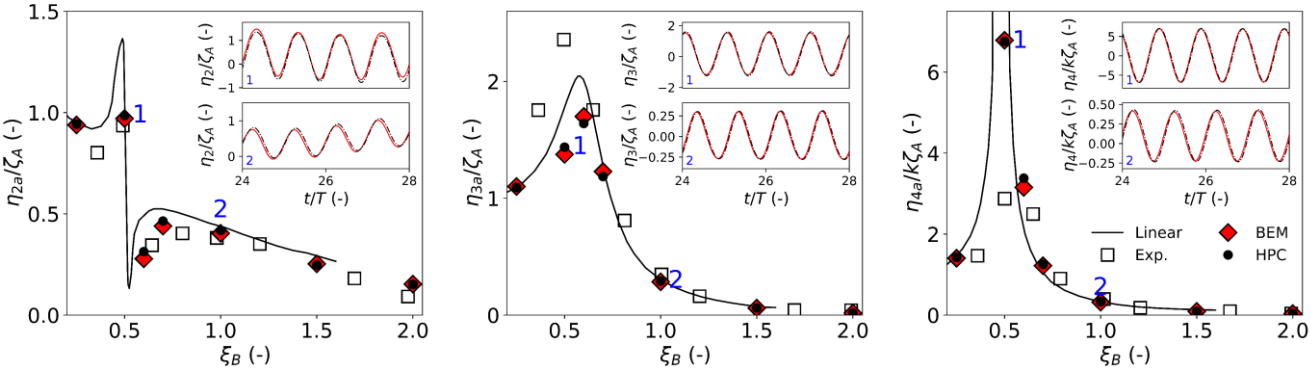

Fig. 2 1st order sway, heave and roll transfer functions versus $\xi_B = kB/2$. k, ζ_A and T are the wave number, amplitude and period of the incident wave. In the time series plots: solid lines = BEM results; dash-dotted lines = HPC results.

Fig. 3 emphasizes the non-linear behavior involved. For frequencies around heave and roll resonance, higher-order loads are non-negligible due to large 1st order motions. For ξ_B = 0.5, the maximum roll motion is close to 30°, meaning that the assumptions of linear theory are violated. On the other hand, the experimental results show

significantly lower roll amplitudes, implying that the viscous damping is significant. For higher wave frequencies, the 2nd order sway and heave force components increase. This might be due to increasing wave non-linearity. For ξ_B = 2.0, $k\zeta_A$ is 0.28, implying significant crest-to-trough asymmetry in the wave elevation.

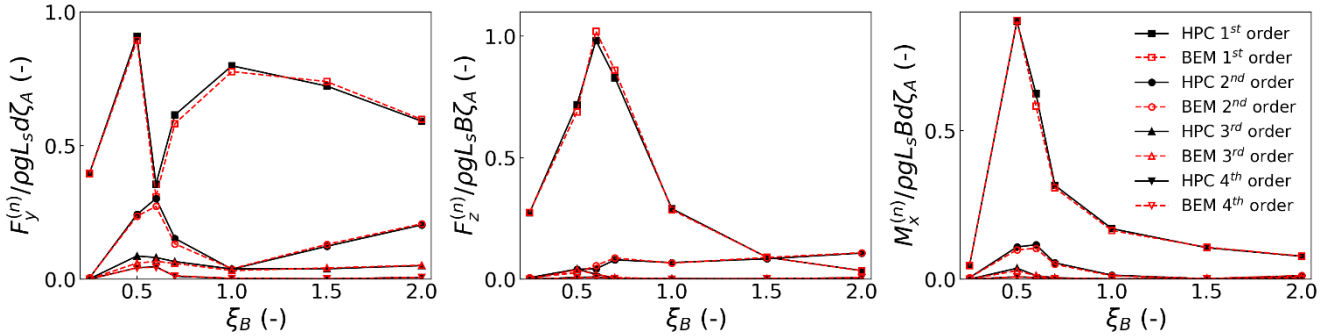

Fig. 3 Transfer functions for 1st-4th order wave loads in sway, heave and roll. L_s is the x-dimension of the ship section, here taken as unity.

To handle scenarios like the resonant conditions examined here, while keeping the advantages of the HPC method, the following DD coupling is proposed. The results will be presented at the workshop.

3 DOMAIN-DECOMPOSITION STRATEGY

Here the LS-NS solver is briefly outlined and the coupling strategy (see Fig. 4) is described. The latter shares the main features of the DD in [2], such as the use of an overlapping region and the reconstruction of the fluid variables, when they are exchanged between the two solvers, so to ensure consistency with the receiver method. However, some aspects of the coupling differ in connection with the use of the HPC method, as explained below.

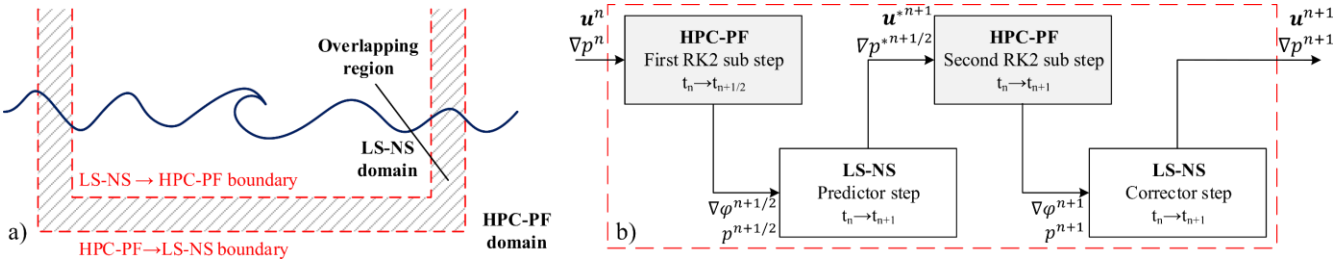

Fig. 4 Spatial a) and temporal b) coupling between HPC-PF and LS-NS solvers.

3.1 Viscous-Flow Solver

To enhance efficiency, the LS-NS solver used here is a single-phase (water) incompressible method as described in [3], where more details and references can be found. The solution of the NS equations is based on a projection method. The spatial discretization is obtained through an Eulerian finite-difference scheme accurate to the 2nd order, with an essentially non-oscillatory (ENO) scheme for the advection terms and a variable-coefficient limiter for the local gradients. The time integration uses a 2nd order predictor-corrector scheme. A LS technique describes the evolution of the air–water interface and bodies inside the fluid domain. The implementation as a single-phase solver is more challenging than for a two-phase flow solver and requires care for an accurate and robust solution across the air-water interface. The air domain is not simulated, and the pressure there is set to zero. This condition is enforced along the air–water interface through a smooth transition from the Poisson pressure equation, inside the water domain, and a Dirichlet condition at the free surface. Moreover, the liquid velocity is extended in the air.

3.2 Spatial Coupling Scheme

The spatial coupling between the two solvers is illustrated in Fig. 4 a). The computational domain is separated into two zones: one where the HPC-PF solver is applied and one where the LS-NS solver is used. The two domains

share an overlapping region, where both solvers are applied. This region allows exchange of information in a more relaxed manner than using a sharp interface. Both solvers use inertial Earth-fixed coordinate systems. In a set of pre-defined points along and near the HPC-PF→LS-NS boundary, the HPC-PF solver gives the fluid velocity vector $\nabla\varphi$ found as the gradient of eq. (1) and the fluid pressure p defined by eq. (2) to the LS-NS solver. In addition, the free-surface elevation is provided at several horizontal locations inside the overlapping region. The LS-NS solver needs information also near its outer edge so to properly reconstruct nearby the fluid gradients and the LS function. In a set of pre-defined points along the LS-NS→HPC-PF boundary, that constitutes the inner edge of the HPC-PF domain, the fluid velocity vector $\boldsymbol{u}$ and the gradient ∇p calculated in the LS-NS solver are given to the HPC-PF solver. These are used to enforce the Neumann boundary conditions for φ and φ_t in the HPC-PF solver.

3.3 Temporal Scheme

The temporal coupling between the two solvers is similar to that in [2]. The scheme is illustrated in Fig. 4 b) for a complete time step from t_n to $t_{n+1} = t_n + \Delta t$, where Δt is the time step, set equal in the two solvers. A 2nd order Runge-Kutta scheme (RK2) is used in the HPC-PF, for the same accuracy order as in the LS-NS. After the first RK2 sub step, the HPC-PF solver computes the fluid velocities and pressure along and near the HPC-PF→LS-NS boundary at $t_{n+1/2}$ and provides these to the LS-NS solver. The LS-NS solver then performs the predictor step, and provides guessed values, denoted with an asterisk, for the fluid velocity at t_{n+1} and fluid pressure gradient at $t_{n+1/2}$ along the LS-NS→HPC-PF boundary. To get ∇p at t_{n+1}, a 2nd-order extrapolation is performed. The second RK2 sub step is then performed and the final HPC-PF solution is obtained at t_{n+1}. Fluid velocities and fluid pressure are computed along and near the HPC-PF→LS-NS boundary and given to the LS-NS solver, that then performs the corrector step to obtain the divergence-free LS-NS solution at t_{n+1}.

ACKNOWLEDGEMENTS

This work has been carried out at the Centre for Autonomous Marine Operations and Systems (AMOS). The Research Council of Norway is acknowledged as the main sponsor of AMOS. This work was partly supported by the Research Council of Norway through the Centre of Excellence funding scheme, Project number 223254-AMOS.

REFERENCES

[1] Hanssen, F. C., Bardazzi, A., Lugni, C., & Greco, M. (2018). Free-surface tracking in 2D with the harmonic polynomial cell method: Two alternative strategies. *International Journal for Numerical Methods in Engineering*, *113*(2), 311-351.

[2] Colicchio, G., Greco, M., & Faltinsen, O. M. (2006). A BEM-level set domain-decomposition strategy for non-linear and fragmented interfacial flows. *International journal for numerical methods in engineering*, *67*(10), 1385-1419.

[3] Colicchio, G., Greco, M., & Faltinsen, O. M. (2011). Domain-decomposition strategy for marine applications with cavity entrapments. *Journal of Fluids and Structures*, *27*(4), 567-585.

[4] Shao, Y. L., & Faltinsen, O. M. (2012, July). Towards efficient fully-nonlinear potential-flow solvers in marine hydrodynamics. In *ASME 2012 31st International Conference on Ocean, Offshore and Arctic Engineering* (pp. 369-380). American Society of Mechanical Engineers.

[5] Ma, S., Hanssen, F. C., Siddiqui, M. A., Greco, M., & Faltinsen, O. M. (2018). Local and global properties of the harmonic polynomial cell method: In-depth analysis in two dimensions. *International Journal for Numerical Methods in Engineering*, *113*(4), 681-718.

[6] Koo, W., & Kim, M. H. (2004). Freely floating-body simulation by a 2D fully nonlinear numerical wave tank. *Ocean Engineering*, *31*(16), 2011-2046.

[7] Nojiri, N. (1980). Study on the Drifting Force on Two-Dimensional Floating Body in Regular Waves. *Transactions of the West-Japan Society of Naval Architects*, 131-152.